AIP | Review of Scientific Instruments

Motional Stark effect diagnostic pilot experiment for MAST

M. Kuldkepp, M. J. Walsh, P. G. Carolan, N. J. Conway, N. C. Hawkes, et al.

Citation: Rev. Sci. Instrum. **77**, 10E905 (2006); doi: 10.1063/1.2220475
View online: http://dx.doi.org/10.1063/1.2220475
View Table of Contents: http://rsi.aip.org/resource/1/RSINAK/v77/i10
Published by the American Institute of Physics.

Motional Stark effect diagnostic pilot experiment for MAST

M. Kuldkepp
Department of Physics, KTH, EURATOM-VR Association, SE-10691 Stockholm, Sweden

M. J. Walsh, P. G. Carolan, N. J. Conway, and N. C. Hawkes
EURATOM/UKAEA Association, Culham Science Centre, Abingdon, Oxfordshire OX14 3DB, United Kingdom

J. McCone
University College Cork, Association EURATOM-DCU, Ireland

E. Rachlew
Department of Physics, KTH, EURATOM-VR Association, SE-10691 Stockholm, Sweden

G. Wearing
EURATOM/UKAEA Association, Culham Science Centre, Abingdon, Oxfordshire OX14 3DB, United Kingdom

(Received 5 May 2006; presented on 9 May 2006; accepted 31 May 2006; published online 27 September 2006)

Exploiting the motional Stark effect (MSE) in the low magnetic fields of spherical tokamaks such as MAST is complicated by the Doppler smearing of the relatively closely spaced Stark components. Extensive modeling of MSE spectra and the subsequent polarized fraction (~20%) of spectrally filtered light and signal to noice ratios have been performed taking account of real experimental conditions including neutral beam parameters, port sizes, optical losses, filter characteristics, etc. A design is selected which uses high throughput interference filters (0.1 nm bandpass) for separation of the spectral components. An accuracy of ~0.5° compared with typically 15° is estimated for field angle measurements. The design allows for early implementation, starting with a pilot two chord system, and for an economic expansion to a multiplicity of chords. Matching the Doppler shifted D_α from the beam neutrals will be accomplished by a combination of filter selection and fine-tuning of the beam voltage. Avoiding filter tuning in the design greatly simplifies the diagnostic. Calibration results of the diagnostic support the calculations. © *2006 American Institute of Physics.* [DOI: 10.1063/1.2220475]

I. INTRODUCTION

The motional Stark effect (MSE) diagnostic has since its discovery[1,2] been an excellent tool for determining the internal magnetic field structure in fusion plasma experiments worldwide.[3–7] The most common MSE diagnostic relies on the fact that the D_α light emitted from a neutral heating beam is polarized and the direction of polarization is related to the direction of the magnetic field. The polarization is attributed to the spectral Stark splitting of the Doppler shifted emission lines due to the Lorentz electric field experienced by the neutral particles as they cross the magnetic field lines. The splitting depends on the velocity of the neutral particles and on the strength of the magnetic field. In MAST the central magnetic field is in the range of 0.3–0.5 T, which typically is much smaller than conventional tokamaks and it follows that the spectral splittings are accordingly smaller. The emission lines are grouped into three categories (π, polarized σ, and unpolarized σ) according to their polarization. It is preferable to only measure on one group but the process of separating the groups is not straightforward in a low field tokamak since the lines typically overlap. In this work we describe a two-channel MSE pilot experiment for MAST. The aim is to determine if it is feasible to use the newly installed neutral heating beam for determination of the internal magnetic field structure. The details of the diagnostic, as well as experimental calibration data, are presented in Sec. II. Section III outlines simulations of the expected performance of the diagnostic.

II. EXPERIMENT

A schematic of the diagnostic is outlined in Fig. 1. It consists of two parts, the collecting part, and the detecting part and they are connected through optical fibers. The collecting part is mounted on a diagnostic port on the MAST vessel and it receives the beam emission through the port window. The light passes through a pair of photoelastic modulators (PEMs) (Hinds PEM-90) and a polarizer sheet (Melles Griot) and is thereafter focused down onto a moulded rectangular fiber bundle by a 38 mm diameter lens. The two fiber bundles have split ends to allow charge-exchange recombination diagnostic fibers to fit in between. Each bundle comprises of thirty-six, 400 μm diameter, numerical aperture (NA)=0.37 (only 0.26 filled) optical fibers and they have a total etendue of 1.1 mm^2 sr which is preserved throughout the diagnostic. The projected area of the beam that each channel covers ranges from 25×100 mm^2 at the

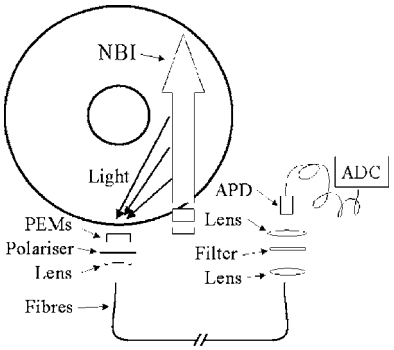

FIG. 1. Schematic diagram of the MAST MSE diagnostic. The collecting part (left) and the detecting part (right) are separated by an optical fiber.

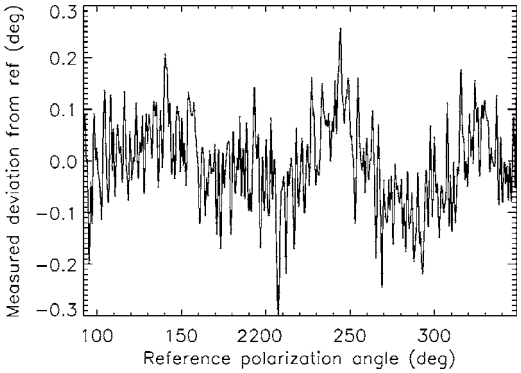

FIG. 2. Remaining error in channel 1 after calibration as a function of angle.

edge of the plasma to 30×140 mm^2 at the plasma center. Both channels can be positioned within the plasma to an accuracy of 0.5 cm by adjusting the physical position of the channel in the image plane. The most important part of the diagnostic is the PEM where the polarization information is decoded into intensity modulations by two rapidly (ω_1 =20 kHz and ω_2=23 kHz) oscillating birefringent crystals.

The detecting part of the diagnostic uses two doublet lenses to expand the beam from the fiber and matches it to a 50 mm diameter, 0.1 nm full width at maximum (FWHM) bandpass, high throughput interference filter (Barr Associates). The interference filter has a two-cavity design to obtain a Gaussian shape at the band edges so that light from other wavelength regions than the measured one will be better suppressed. The fiber bundle on the detecting part has a circular cross section to minimize the spread of angles illuminating the filter. Nevertheless, due to the finite size of the fiber bundle the spread of angles seen by the filter will increase its FWHM to 1.04 Å. After passing through the lens the light is focused by a doublet lens onto an avalanche photodiode (APD) (Hamamatsu C5460-01) with an active area with 3 mm diameter and 100 kHz cut-off frequency. The electrical signal is thereafter measured at 250 kHz and stored by an analog to digital (ADC) card for further digital processing.

The system has been bench calibrated using a polarizer attached to a rotating stage (Newport RV120) to determine the response to all linear polarization angles. Two opal diffusers have been put in front of the tungsten light source to ensure that the light is completely unpolarized before passing through the polarizer. The rotator indicates its position to within an accuracy of 0.01° and is used as a reference to determine the deviation from measured and actual polarization. Digital lock-in methods have been used to determine different harmonics of the intensity variations created by the PEMs.[8] The measured polarization angle can, for equal drive amplitude of the PEMs, be approximated by

$$\gamma_m = \frac{1}{2}\arctan\left(\frac{V_{2\omega_2}}{V_{2\omega_1}}\right), \tag{1}$$

where $V_{2\omega_2}$ is the detected signal of the frequency component at two times ω_2 and $V_{2\omega_1}$ at two times ω_1. For better accuracy it is necessary to obtain the full Stokes vector representation of light through simultaneous inversion of several signals (dc signal, $V_{2\omega_2}$, $V_{2\omega_1}$, and V_{ω_1}) and to measure and compensate for individual drive amplitudes. From the deviation between measured and reference polarizations it has been possible to determine that the analyzing polarizer after the PEMs is misaligned by 1.5°. After digital compensation for this, higher order errors and noise contribute to less than an overall error of ±0.1° at 15 ms time resolution as is shown in Fig. 2. The polarization fraction during calibration is 100% which is higher than the 20% (see Sec. III) anticipated during experiments, but the intensity is only 5×10^{-10} W which is much lower than the predicted 80×10^{-10} W at the center of the plasma during plasma operation.

The common procedure to tune the wavelength of an interference filter is by tilting it. This will not be done on MAST since tilting the filter would increase its FWHM unacceptably. Instead in order to reach the desired spectral position a suitable filter will be selected (four filters with different peak transmission wavelengths are presently available) and the position fine-tuned using the beam voltage. The beam voltage can be stepped in units of keV, meaning steps of roughly 0.03 nm for the present geometry and a 60 keV beam.

III. SIMULATIONS

Prior to the construction of the diagnostic, extensive simulations were carried out to establish the performance of different potential systems. A code has been developed that numerically calculates the MSE spectrum including spectral broadening effects such as beam divergence, finite collection volume, filter bandpass shape, beam voltage ripple, and collection optics size. The divergence of the beam is an important broadening mechanism on MAST and the beam divergence has been determined to be 1.2° by measuring the shape of the Doppler shifted beam emission spectra from test runs (no magnetic field). The simulated spectrum is gradually built up by adding contributions from all beam positions in the field of view. The resulting spectrum from a simulation with a 60 keV neutral beam and a central toroidal magnetic field of 0.5 T is shown in Fig. 3(a). The different components (π, polarized σ, and unpolarized σ) overlap spectrally and it is not possible to separate individual polarizations. However, in the figure the three groups have been plotted separately to show qualitative differences. It is possible to see that the shape of the π group is much broader than the σ light and it is also possible to see that the unpolarized σ has little effect

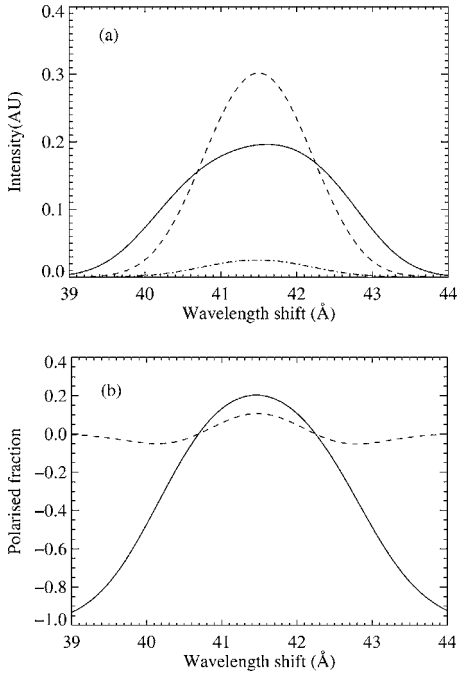

FIG. 3. (a) Simulated spectrum for plasma core showing π (full), polarized-σ (dashed), and unpolarized-σ (dash dotted) beam emissions. (b) Polarized fraction (full) and polarized intensity (dashed) of beam emission.

on the spectrum as most of the power lie in the polarized σ. From Fig. 3(a) it is possible to determine the expected polarized fraction [polarized fraction$=(I_{\sigma\text{pol}}-I_{\pi})/I_{\text{tot}}$] of the light and how much polarized light (polarized intensity$=I_{\sigma\text{pol}}-I_{\pi}$) is collected [Fig. 3(b)]. The polarized fraction is a function of both plasma radius and spectral position. At the plasma core the polarized fraction is expected to be $\sim$20% at the spectral center (σ light) and close to unity at the edges (π light). The benefit of using σ light is that the same setting can then be used for any magnetic field. Furthermore, although measuring π light would increase the polarized fraction it is done at the cost of losing intensity, as can be seen from the drop in polarized intensity. As the polarized fraction depends on the toroidal field, it gradually decreases with radius from 20% at the core to 9% at the outer plasma edge. For a lower on axis toroidal field (0.3 T), the polarized fraction drops from 8% (plasma core) to 2% (plasma edge) and it is therefore possible that π light has to be used instead of σ light for low fields. For signal to noise calculations both the polarized fraction and the fraction of light collected are important. Using the radial profile of the polarized fraction (on axis toroidal field of 0.5 T) and including information from a separate code[9] that predicts the D_{α} beam emission along the line of sight, the expected signal to noise ratio can be calculated and the noise in polarization angle anticipated for a time resolution of 1 ms is shown in Fig. 4. The noise in the pitch angle at the center of the plasma ($R\approx 83$ cm) is slightly higher than 0.3°. The large increase in noise towards the center is connected to the gradual ionization of beam neutrals as they penetrate into the plasma. The systematic error of the

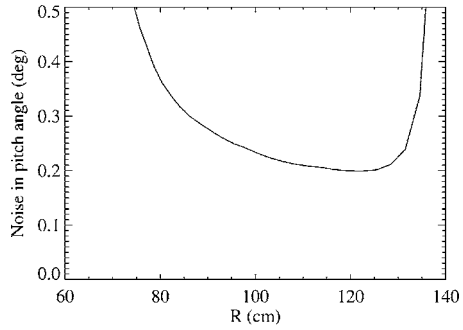

FIG. 4. Simulation of noise in measured polarization angle as a function of plasma radius.

diagnostic due to unknown rotations of the PEM transmission axis with respect to the torus is expected to be of the order of 0.2°, giving a total anticipated error in the pitch angle less than $\sim$0.5°. To obtain higher accuracy the time resolution could be decreased to 10 ms (giving pitch angle noise better than 0.1°) and calibration methods such as beam into gas or using an in-vessel calibration rig are planned to decrease the systematic error. Under those constraints it will be possible to run the MAST MSE diagnostic with a pitch angle noise $\sim$0.2° which is similar to what is seen for the JET MSE system.[10] Even at the edge the emission from a 60 keV beam has enough Doppler shift that emission from polluting carbon lines is not expected to influence the spectra. A simulation run for the calibration condition yields an expected noise level of 0.07°, which is somewhat smaller than is seen (Fig. 2) but still close enough to benchmark the simulator. The simplicity of the design will make extension into several channels straightforward and it is expected that a multichannel system will be tunable. Although two channels are not enough to determine the q profile, they are expected to help constrain it at important positions in the plasma and experiments are already planned where the two-channel MSE system will yield important plasma physics results.

ACKNOWLEDGMENTS

This work is funded jointly by the U.K. Engineering and Physical Sciences Research Council and EURATOM.

[1] F. M. Levinton, R. J. Fonck, G. M. Gammel, R. Kaita, H. W. Kugel, E. T. Powell, and D. W. Roberts, Phys. Rev. Lett. **63**, 2060 (1989).
[2] A. Boileau, M. von Hellermann, W. Mandl, H. P. Summers, H. Weisen, and A. Zinoviev, J. Phys. B **22**, L145 (1989).
[3] D. Wroblewski and L. Lao, Rev. Sci. Instrum. **63**, 5140 (1992).
[4] F. M. Levinton, Rev. Sci. Instrum. **63**, 5158 (1992).
[5] B. C. Stratton, D. Long, R. Palladino, and N. C. Hawkes, Rev. Sci. Instrum. **70**, 898 (1999).
[6] D. Craig, D. J. Den Hartog, G. Fiksel, V. I. Davydenko, and A. A. Ivanov, Rev. Sci. Instrum. **72**, 1008 (2001).
[7] K. Jakubowska, M. De Bock, R. Jaspers, M. Von Hellermann, and L. Shmaenok, Rev. Sci. Instrum. **75**, 3475 (2004).
[8] M. Kuldkepp, N. C. Hawkes, E. Rachlew, and B. Schunke, Appl. Opt. **44**, 5899 (2005).
[9] M. Tournianski, Ph.D. thesis, University of Essex, 1999.
[10] N. C. Hawkes, K. Blackler, B. Viaccoz, C. H. Wilson, J. B. Migozzi, and B. C. Stratton, Rev. Sci. Instrum. **70**, 894 (1999).